Mechanical Systems and Signal Processing 41 (2013) 348–356

Contents lists available at ScienceDirect

Mechanical Systems and Signal Processing

journal homepage: www.elsevier.com/locate/ymssp

Singular value decomposition based feature extraction approaches for classifying faults of induction motors

Myeongsu Kang, Jong-Myon Kim *

School of Electrical Engineering, University of Ulsan, Ulsan, South Korea

ARTICLE INFO

Article history:
Received 19 November 2012
Received in revised form
1 August 2013
Accepted 2 August 2013
Available online 22 August 2013

Keywords:
Fault classification
Feature extraction
Induction motor
Short-time energy
Singular value decomposition
Support vector machine

ABSTRACT

This paper proposes singular value decomposition (SVD)-based feature extraction methods for fault classification of an induction motor: a short-time energy (STE) plus SVD technique in the time-domain analysis, and a discrete cosine transform (DCT) plus SVD technique in the frequency-domain analysis. To early identify induction motor faults, the extracted features are utilized as the inputs of multi-layer support vector machines (MLSVMs). Since SVMs perform well with the radial basis function (RBF) kernel for appropriately categorizing the faults of the induction motor, it is important to explore the impact of the σ values for the RBF kernel, which affects the classification accuracy. Likewise, this paper quantitatively evaluates the classification accuracy with different numbers of features, because the number of features affects the classification accuracy. According to the experimental results, although SVD-based features are effective for a noiseless environment, the STE plus SVD feature extraction approach is more effective with and without sensor noise in terms of the classification accuracy than the DCT plus SVD feature extraction approach. To demonstrate the improved classification of the proposed approach for identifying faults of the induction motor, the proposed SVD based feature extraction approach is compared with other state-of-the art methods and yields higher classification accuracies for both noiseless and noisy environments than conventional approaches.

1. Introduction

Industrial processes need to be monitored in real time based on the input–output data observed during their operation. Abnormalities in an induction motor should be detected early in order to avoid costly breakdowns. The induction motor is widely used in industrial manufacturing, and its failures can result in significant economic losses. However, the growing scale of industrial processes involving induction motors has complicated the diagnosis and isolation of both electrical and mechanical faults of induction motors. Therefore, several approaches have been proposed for detecting faults in an induction motor system [1,2].

For the fault detection and classification of the induction motor, many researchers have mainly utilized current and voltage signals that can be easily measured. They have also used vibration signals for fault detection and classification since vibration signals are more effective at assessing a machine's status than current or voltage signals, even though vibration

* Correspondence to: Bldg. #7, Room #308, 93 Daehak-ro Mugeo-dong, Nam-gu, Ulsan 680-749, South Korea. Tel.: +82 52 259 2217; fax: +82 52 259 1687.
E-mail addresses: ilmareboy@gmail.com (M. Kang), jongmyon.kim@gmail.com, jmkim07@ulsan.ac.kr (J.-M. Kim).

0888-3270/$ - see front matter © 2013 Elsevier Ltd. All rights reserved.
http://dx.doi.org/10.1016/j.ymssp.2013.08.002

signals have non-deterministic and non-stationary characteristics [3]. Furthermore, vibration monitoring is the most reliable method of assessing the overall health of a rotor system [4]. For these reasons, this paper uses the vibration signals of the induction motor to classify faulty data from normal data.

Vibration signals are analyzed in the time, frequency, and time-frequency domains, and features are extracted using these analyses [5–7]. In this paper, we analyze the vibration signals of the induction motor in both the time and frequency domains and propose robust feature extraction methods to achieve high classification accuracy even in a noisy environment: one uses a short-time energy (STE) plus singular value decomposition (SVD) technique through the time-domain analysis, and another utilizes a discrete cosine transform (DCT) plus SVD technique with the frequency-domain analysis. We then use them as the inputs of the classifiers for the fault classification of the induction motor.

There are a number of classifier models for fault classification, such as analytical model-based methods and artificial intelligence-based methods (e.g., knowledge-based models and data-based models) [8–10]. Although analytical- and knowledge-based models are effective, they have low classification accuracy for the induction motor because they lack adaptability and are poorly suited to the random nature of vibration signals [10]. Some popular data-based models are used for detecting and classifying faults of the induction motor: neural networks, fuzzy systems, and support vector machines (SVM). This paper employs SVMs as classifiers since they provide better properties than other models, and they can also offer high classification performance with a limited training dataset. However, when SVMs are employed for classification, we need to select an effective kernel for the SVM. This paper utilizes the radial basis function (RBF) kernel, which performs better with SVMs. In this case, it is important to find both an optimal number of features and a value of standard deviation (σ) for the RBF, since these can strongly affect the classification accuracy. Thus, this paper measures the classification accuracy with different numbers of features and σ values for the RBF kernel in order to scrutinize the impacts of these factors on the fault classification.

The rest of this paper is organized as follows. Section 2 introduces related research, and Section 3 presents the data acquisition environment and a brief description of induction motor faults. In Section 4, the two proposed feature extraction methods are described, and Section 5 introduces multi-layer SVMs (MLSVMs) for fault classification of the induction motor. Section 6 shows the classification performance with different numbers of features and σ values for the radial basis function (RBF) kernel, as well as the performance improvement of the proposed approach, and Section 7 concludes this paper.

2. Related works

As mentioned in Section 1, vibration signals can be analyzed in the time, frequency, and time-frequency domains, and features are extracted through these analyses for identifying multiple faults in the induction motor [5–7,11,12]. Many researchers have utilized statistical values (e.g., mean, variance, root-mean-square, and kurtosis) and spectral powers using time and frequency analyses, respectively [5,11,12]. Moreover, statistical values using the short-time Fourier transform, discrete wavelet transform (DWT), and mel-frequency cepstral coefficients through a time-frequency analysis have been employed [5,6,11,13–15], and these features are suitable for most mechanical systems. The features (kurtosis, mean, and variance using DWT) in [11], for example, represent the characteristics of bearing faults well. As shown in Fig. 1(a) and (b), however, kurtosis- and mean-based features are less effective for classifying the faults of the induction motor due to irregular patterns with features, which lead to low classification accuracy. In addition, most of the extracted features are overlapped with the others, as depicted in Fig. 1(a) and (b), which results in difficulties in identifying the induction motor faults. To solve this problem, we propose efficient SVD-based feature extraction methods for distinguishing faults in the induction motor.

3. Faults of an induction motor

The experimental setup used in this study consists of pulleys, a belt, shaft, fan, and a 4-pole three phase induction motor, which operates at 0.5 kW, 220 V, and 3560 revolutions per minute, as shown in Fig. 2(a). Four induction motors were utilized to produce the data needed under full-load and steady-state conditions. One of the motors is healthy, and is considered as a baseline to discriminate from those with faults, including broken rotor bars, bowed rotor, bearing outer race

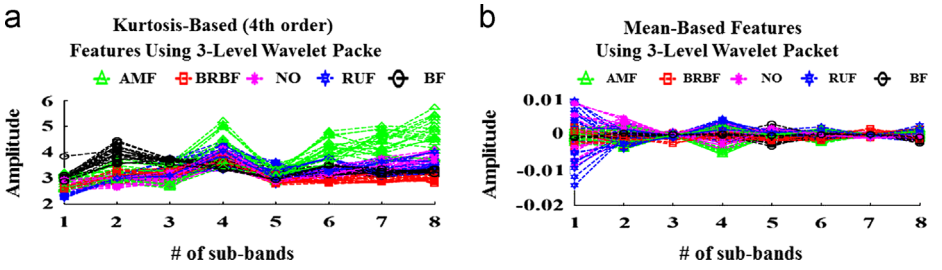

Fig. 1. Feature extraction results for classifying faults of the induction motor using the methods in [11]. (a) Fourth-order kurtosis-based features using a 3-level wavelet packet and (b) mean-based features using a 3-level wavelet packet.

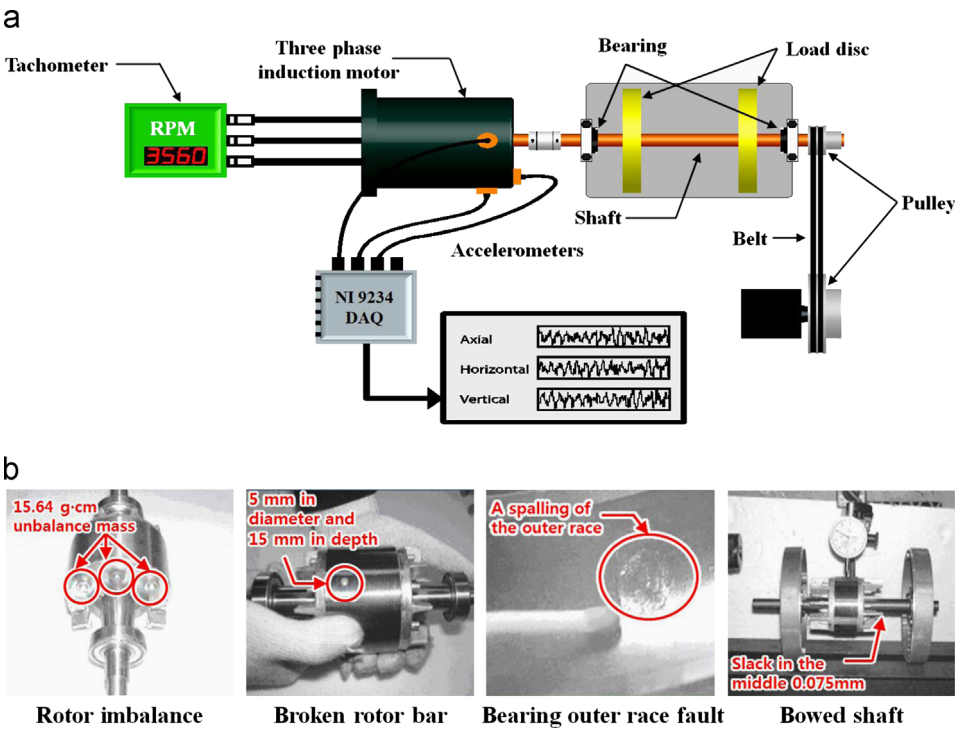

Fig. 2. Self-defined test rig for the experimental setup (a) and faulty induction motors (b).

Table 1
Description of faults of the induction motor.

Type of faults	Fault description
Angular misalignment fault (AMF)	Angular misalignment is effective between the two shaft centerlines, where the angle between the shaft centerlines is 0.48° in this study
Broken rotor bar fault (BRBF)	12 of 34 rotor bars are involved in the plastic deformation of the grinding furrow as depicted in Fig. 2(b): 5 mm in diameter and 15 mm in depth
Normal (NO)	The induction motor is normal (or healthy)
Rotor unbalance fault (RUF)	Unbalance mass of 15.64 g cm is added at the right end of the rotor as shown in Fig. 2(b)
Bearing fault (BF)	A spalling on the outer race of the bearing is replicated as presented in Fig. 2(b)
Bowed shaft fault (BSF)	The shaft is slack in the middle (0.075 mm), which causes dynamic air-gap eccentricity
Parallel misalignment fault (PMF)	Parallel misalignment is the effective perpendicular distance between the two shaft centerlines and the distance between the shaft centerlines is 15 mm in this study

fault, rotor unbalance, adjustable eccentricity motor (e.g., angular misalignment), as illustrated in Fig. 2(b). Especially, three induction motor faults (e.g., angular misalignment, parallel misalignment, and rotor unbalance) were produced with the normal induction motor. Therefore, seven different vibration signals, including normal (or healthy) ones, were employed for fault classification for the induction motor. Table 1 presents a brief description of each fault. In addition, the vibration signals were acquired from accelerometers located in the axial, horizontal, and vertical directions of the motor bearing housing and the acquired vibration signals were sampled at 8,000 Hz. In this study, 105 one-second-long vibration signals from the axial accelerometer for each condition were utilized, which well represents the fault characteristics of the induction motor.

4. SVD-based feature extraction methods

To early identify induction motor faults in this study, vibration signals can be analyzed in either the time or frequency domain, and the features are extracted through these analyses. This paper analyzes seven different vibration signals in both the time and frequency domains and proposes two SVD-based feature extraction methods: the STE plus SVD technique in the time-domain analysis, and the DCT plus SVD technique in the frequency-domain analysis.

4.1. Singular value decomposition

SVD is a general linear algebra technique that is used to analyze matrices. A matrix X of size $n \times n$ can be represented by its SVD, as defined by

$$X = U \times S \times V^T, \tag{1}$$

where U is an $n \times n$ orthogonal matrix, V is an $n \times n$ orthogonal matrix, and S is an $n \times n$ matrix with the diagonal elements representing the singular values, $\sigma_1 > \sigma_2 > \cdots > \sigma_n$, of X [16]. The matrix S is represented as follows:

$$X = U \times S \times V^T = [u_1, u_2, ..., u_n] \times \begin{bmatrix} \sigma_1 & & & 0 \\ & \sigma_2 & & \\ & & \ddots & \\ 0 & & & \sigma_n \end{bmatrix} \times [v_1, v_2, ..., v_n] = \sum_{i=1}^{n} u_i \sigma_i v_i^T. \tag{2}$$

The columns of the orthogonal matrix U are called the *left singular* vectors, and the columns of the matrix V are called the *right singular* vectors. The *left singular* vectors of X are the eigenvectors of XX^T, and the *right singular* vectors are the eigenvectors of X^TX. Vibration signals are generally obtained from vibration sensors such as accelerometers, and noise components can be consequently included in the acquired vibration signals, and are generally called *sensor noise*. This can cause difficulties in feature extraction as well as low classification accuracy. The vibration signal and the noise signal, which is white Gaussian, have low cross-correlation, and this paper utilizes singular value decomposition to partition the noise components by keeping larger entries of singular values. This technique basically removes the low-power, i.e., noise, portion of the vibration signal. Consequently, SVD might be a promising technique to minimize the effect of noise components inherent in vibration signals when we extract features and identify the faults of the induction motor. More details will be given in Section 4.4.

4.2. Short-time energy plus singular value decomposition feature extraction

This paper proposes a feature extraction method combining short-time energy (STE) with the singular value decomposition (SVD) technique to distinguish faults in the induction motor. STE is a simple feature that is used in a wide variety of classification schemes [17,18], and it is calculated as follows:

$$STE = \sum_{i=0}^{N-1} x^2(i), \tag{3}$$

where N is the total number of samples in the processing window, and $x(i)$ is the value of the ith sample. Fig. 3 shows the patterns of 10 STE values from 20 vibration signals that were randomly selected among 105 vibration signals for each type of fault, including no-fault scenarios. As depicted in Fig. 3, although STE values can be good features to distinguish several faults from normal ones, some STE values overlap with others (between AMF and NO, between BRBF and PMF, and so on). Furthermore, irregular patterns of the STE values can lead to low classification accuracy. Consequently, we propose a new STE plus SVD-based feature extraction method to solve these problems. Fig. 4 presents the feature extraction process and the features extracted using the proposed method.

Fig. 4(a) illustrates the feature extraction process using the STE plus SVD technique. It consists of the following three steps:

- *Step* 1*:* A one-second long input signal is divided into $N_{feature} \times N_{feature}$ sub-bands, and the STE values are calculated in each sub-band using Eq. (3), where $N_{feature}$ is the number of features to be extracted.
- *Step* 2: Constructs a new $N_{feature} \times N_{feature}$ matrix that is composed of the STE values computed in *Step* 1.
- *Step* 3: Decompose the $N_{feature} \times N_{feature}$ matrix using SVD and use the ($N_{feature}$-3) singular values as features to categorize the faults of the induction motor.

Similar to Fig. 3, Fig. 4(b) demonstrates 10 singular values for 20 vibration signals selected from among 105 vibration signals for each type of fault. More regular patterns are shown with singular values compared to STE values in Fig. 3, and this

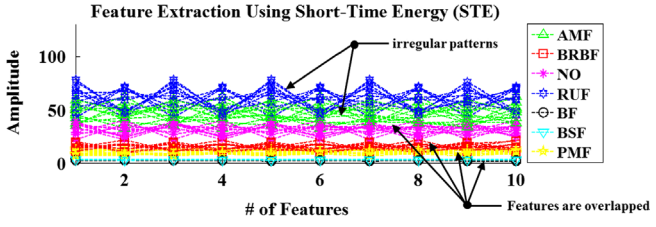

Fig. 3. Patterns of 10 STE values for 20 vibration signals for each type of faulty data and the normal signal.

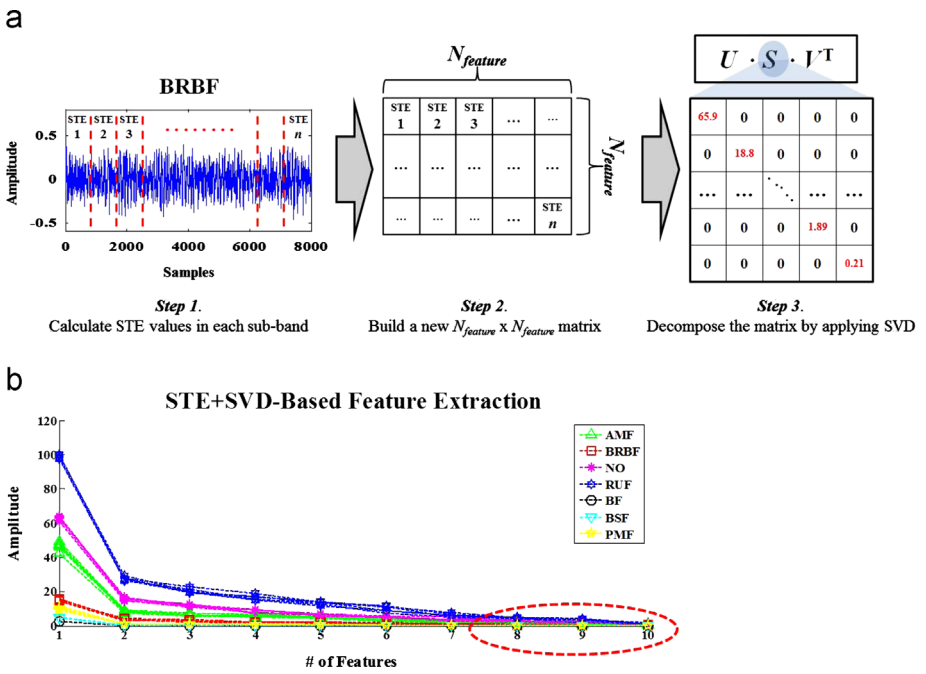

Fig. 4. Feature extraction process and extracted features using the proposed method. (a) STE plus SVD-based feature extraction process, and (b) features using the STE plus SVD techniques.

can result in better classification performance. Moreover, this paper selects ($N_{feature}$-3) singular values as features of the induction motor faults. This is because most of the last three singular values overlap with others as shown in Fig. 4(b), which causes low classification accuracy. Likewise, we remove the effects of the low-power sensor noise that is inherent in acquired vibration signals by using larger ($N_{feature}$-3) singular values.

4.3. Discrete cosine transform and singular value decomposition

In addition to the STE plus SVD-based feature extraction method, this paper also proposes another feature extraction method using the discrete cosine transform (DCT) plus SVD technique as the frequency-domain analysis. DCT is a technique that converts a signal into elementary frequency components [19], and it is widely used because of its energy compaction and decorrelation properties. The transformed matrix consists of DC and AC coefficients, where the first element in the DCT transformed matrix, which is the most significant coefficient, is called a DC coefficient. The remaining coefficients are less important AC coefficients, which are calculated as follows:

$$Y(0) = \frac{\sqrt{2}}{N}\sum_{i=0}^{N-1} x(i),$$

$$Y(k) = \frac{\sqrt{2}}{N}\sum_{i=0}^{N-1} x(i)\cos\left(\frac{(2i+1)k\pi}{2N}\right), \quad k = 1, 2, \ldots, (N-1), \tag{4}$$

where N is the total number of samples in the processing window, $x(i)$ is the value of the ith sample, $Y(0)$ is a DC coefficient, and $Y(k)$ are the AC coefficients.

To find appropriate features that yield high classification performance, we utilize DC coefficients with the SVD technique. The feature extraction process is analogous to the process in Fig. 4(a). In *Step* 1 of Fig. 4(a), we calculate the DC coefficients instead of STE values, and build a new $N_{feature} \times N_{feature}$ matrix. Similar to the STE plus SVD feature extraction, DCT plus SVD-based features are sufficient for classifying faults of the induction motor, and we also utilize ($N_{feature}$-3) DCT plus SVD-based features for classification.

4.4. Robustness in noisy environments

As mentioned in Section 3, vibration signals may include noise components, which are generally called *sensor noise* and are usually considered to be white Gaussian noise, resulting in low classification accuracy. Fig. 5 illustrates an example of STE plus SVD-based features after the embedding of white Gaussian noise. In the experiments, we insert white Gaussian noise into the acquired vibration signals and set the signal-to-noise ratio (SNR) between the vibration signals and the

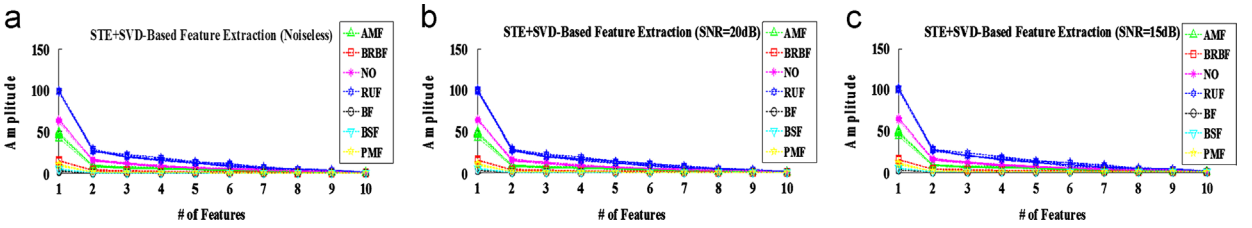

Fig. 5. Feature extraction results using STE plus SVD techniques with or without noise addition. (a) Features without noise addition, and features with noise addition (b) SNR=20 dB, and (c) SNR=15 dB.

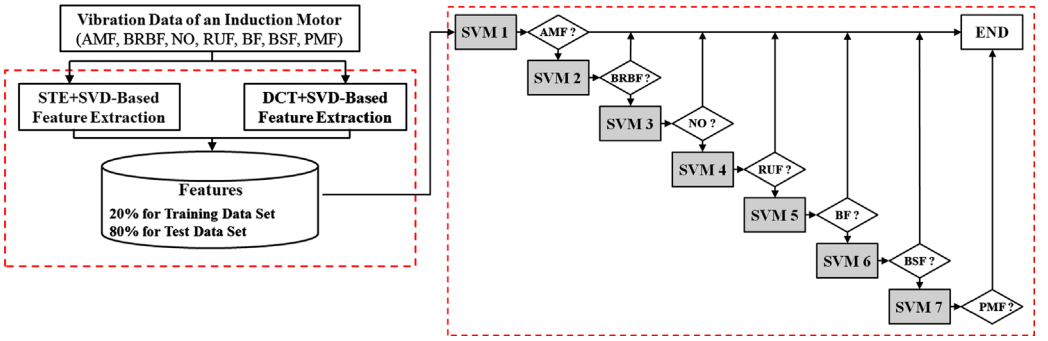

Fig. 6. Fault classification of the induction motor using multi-layer SVMs.

noise-inserted signals to 15 dB and 20 dB. As shown in Fig. 5, the proposed SVD-based feature extraction approach can be effective, even in noisy environments.

5. Multi-layer support vector machines

This section presents multi-layer support vector machines (MLSVMs) for fault classification. The standard SVM is a non-probabilistic binary classifier that can analyze data and recognize patterns [20]. SVMs are also capable of learning in high-dimensional spaces and can provide high performance with a limited training dataset. The basic principle of the SVM classifier is to use a hyper-plane to divide a given dataset into two classes while maximizing the margin. In many applications, however, there are a number of datasets that cannot be linearly separated. There is likely no hyper-plane that can split the non-linear datasets into two classes. To deal with these problems, a soft margin SVM or a kernel is used. We employ SVM to classify faulty signals of the induction motor into seven different categories (AMF, BRBF, NO, RUF, BF, BSF, and PMF) and utilize the RBF kernel to map the inputs to a high-dimensional feature space. This is because SVM performs better with the RBF than with other kernels [21]. The RBF kernel is represented as follows:

$$k(x,y)=\exp\left(-\frac{\|x-y\|^2}{2\sigma^2}\right), \tag{5}$$

where $k(x, y)$ is the RBF kernel, x and y are the input feature vectors, and σ is a parameter established by the user to determine the width of the effective basis kernel. If small σ values are used, overtraining occurs, so that the basis function is wrapped tightly around the data points. In contrast, if large σ values are used, the basis function draws an oval around the points without defining their shape or pattern [21]. Consequently, the σ values can affect the classification performance, so we select optimal σ values to identify induction motor faults.

As mentioned before, the SVM is designed to separate the data into only two classes. As a consequence, we need multi-layer SVMs (MLSVMs) to classify the faults of the induction motor. Fig. 6 shows the MLSVMs that are used to categorize the faults of the induction motor in this study.

SVM1–SVM7 classify data as an angular misalignment fault (AMF), broken rotor bar fault (BRBF), normal (NO), rotor unbalance fault (RUF), bearing fault (BF), bowed shaft fault (BSF), and parallel misalignment fault (PMF), in that order. To test and train the MLSVMs, we build a test dataset with 80% of the 105 vibration signals for each fault, including normal ones, and a training dataset with the remaining signals (i.e., 84 one-second-long vibration signals are used as the test dataset, and 21 one-second vibration signals are used as the training data).

6. Classification results

This paper proposes two feature extraction methods: the STE plus SVD-based technique and the DCT plus SVD-based technique. These extracted features are then passed to the MLSVMs for fault classification. As mentioned in Section 1, although both the σ values of the RBF kernel, which determines the width of the effective basis kernel, and the number of features for identifying the induction motor faults can affect the classification performance, no general consensus has been reached as to which values of ($N_{feature}$-3) and σ provide the maximum classification performance. Furthermore, it is not a simple problem to select specific values of ($N_{feature}$-3) and σ that offer high classification accuracy for different types of failures, different types of machines, and different types of signals, because the optimal values of ($N_{feature}$-3) and σ can be changed according to the following reasons:

- If we utilize different types of signatures of induction motor faults (not STE plus SVD and DCT plus SVD based features), we may have to reselect the optimal values of ($N_{feature}$-3) and σ in order to achieve high classification accuracy.
- Although we utilize STE plus SVD and DCT plus SVD based features for identifying induction motor faults, the magnitudes of these features can vary with the acquired signals (e.g., vibration signal, current signal, and acoustic emission signal). This means that different values of ($N_{feature}$-3) and σ should be used for classifying faults and distinguishing them from healthy scenarios.
- Sensors (e.g., different types of accelerometers or different types of current sensors) may cause magnitude variations in the faulty signatures. This results in re-optimizing the values of ($N_{feature}$-3) and σ for high classification performance.

Thus, we experimentally select the optimal values of ($N_{feature}$-3) and σ for our datasets to provide high classification performance. To explore the impacts of these factors, we measure the classification performance with σ values that range from 0.3 to 1 with different numbers of features, where the number of features ($N_{feature}$-3) ranges from 5 to 10 (e.g., $N_{feature}$ is in the range from 8 to 13). Due to the limited number of pages, more details about the experimental results to estimate the

Table 2
Optimal σ values of each support vector machine for STE plus SVD and DCT plus SVD feature extraction approaches.

Type of faults	Optimal σ values for achieving high classification accuracy	
	STE plus SVD	DCT plus SVD
SVM 1 for identifying AMF	0.65	0.85
SVM 2 for identifying BRBF	0.8	0.9
SVM 3 for identifying NO	0.65	0.55
SVM 4 for identifying RUF	0.3	0.3
SVM 5 for identifying BF	0.55	0.95
SVM 6 for identifying BSF	0.3	0.45
SVM 7 for identifying PMF	0.3	0.3

Table 3
Classification accuracy in terms of true positive in a noiseless environment.

Comparison algorithms		Classification accuracy in terms of true positive							Average
		AMF	BRBF	NO	RUF	BF	BSF	PMF	
Algorithm 1 [22]	TP rate (%)	91.35	91.54	84.23	90.38	96.73	98.46	80.19	90.41
Algorithm 2 [23]	TP rate (%)	100.00	89.81	92.31	98.27	100.00	100.00	100.00	97.20
STE+SVD	TP rate (%)	100.00	100.00	100.00	100.00	100.00	85.71	100.00	97.96
DCT+SVD	TP rate (%)	100.00	100.00	97.62	100.00	100.00	81.00	100.00	96.95

Table 4
Classification accuracy in terms of true positive in a noisy environment, SNR=20 dB.

Comparison algorithms		Classification accuracy in terms of true positive							Average
		AMF	BRBF	NO	RUF	BF	BSF	PMF	
Algorithm 1 [22]	TP rate (%)	91.54	88.08	84.04	90.96	95.96	99.04	79.81	89.92
Algorithm 2 [23]	TP rate (%)	99.81	87.88	82.12	93.85	100.00	97.12	100.00	94.40
STE+SVD	TP rate (%)	100.00	100.00	100.00	100.00	100.00	85.71	100.00	97.96
DCT+SVD	TP rate (%)	100.00	100.00	97.62	100.00	100.00	81.00	100.00	96.95

Table 5
Classification accuracy in terms of true positive in a noisy environment, SNR=15 dB.

Comparison algorithms		Classification accuracy in terms of true positive							Average
		AMF	BRBF	NO	RUF	BF	BSF	PMF	
Algorithm 1 [22]	TP rate (%)	91.45	88.00	84.00	90.91	96.00	98.91	79.82	89.87
Algorithm 2 [23]	TP rate (%)	100.00	88.60	74.61	89.81	100.00	88.46	99.81	91.61
STE+SVD	TP rate (%)	100.00	100.00	100.00	100.00	100.00	84.52	100.00	97.79
DCT+SVD	TP rate (%)	100.00	100.00	100.00	100.00	97.62	67.86	100.00	95.07

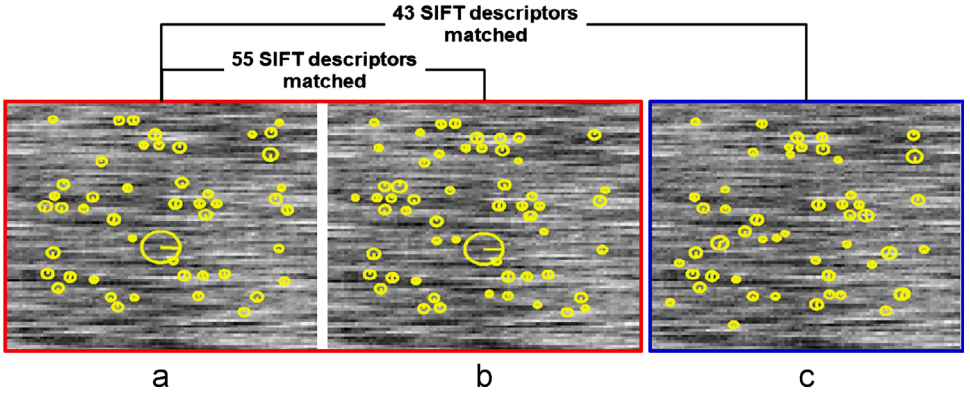

Fig. 7. Variation of SIFT descriptors in (a) a noiseless environment, (b) a noisy environment (SNR=20 dB), and (c) a noisy environment (SNR=15 dB).

optimal values of ($N_{feature}$-3) and σ are available at http://eucs.ulsan.ac.kr/MSSP/2012/IMFD. According to our experiments, the highest classification accuracies were achieved when the ($N_{feature}$-3) values of the STE plus SVD and DCT plus SVD based features were 9 and 8, respectively. In addition, the optimal σ values for each support vector machine are presented in Table 2.

In this study, the classification accuracy is defined with respect to the true positive, which is the number of faults in category i that are correctly classified into category i (e.g., category 1 for AMF, category 2 for BRBF, category 3 for NO, category 4 for RUF, category 5 for BF, category 6 for BSF, and category 7 for PMF). To demonstrate the improved accuracy of the proposed approach for identifying the faults of the induction motor, the proposed approach is compared with other state-of-the-art methods. Tables 3–5 show the classification accuracies for both noiseless and noisy environments. Algorithm 1 [22] utilized the time-domain features from the vibration signals such as statistical features (e.g., root mean square, variance and skewness) to ensure a low computational burden, and then classified the bearing-related faults in the induction motor by employing the neural network as a classifier. Although Algorithm 1 achieved high classification accuracies for both noiseless and noisy environments, the classification accuracies for BRBF, NO, RUF and PMF were relatively lower than those of AMF, BF, and BSF in noisy environments, since the characteristic information of BRBF, NO, RUF, and PMF were not distinctive for identifying these induction motor failures. Consequently, the extracted features moved from one category to another. Algorithm 2 [23] translated an input vibration signal into a gray-level image for the fault classification of the induction motor, and extracted a 128-dimension feature vector that contains the information of the key point descriptors of the image: locations, weights, and orientations. To identify the induction motor faults, the authors calculated the Euclidean distances between the extracted feature vector and each of the centroid feature vectors in the text of the dictionary. The authors then determined the centroids that yielded the minimum Euclidean distance. Despite the fact that Algorithm 2 also achieved high classification accuracy in the noiseless environment, it resulted in low classification accuracies in noisy environments due to the global changes of the scale-invariant feature transform (SIFT) descriptors, as shown in Fig. 7. In contrast, the proposed approached offers higher classification accuracies than Algorithms 1 and 2 in noisy environments.

7. Conclusions

To detect rapidly and classify the faults of the induction motor, this paper proposed two feature extraction methods: STE plus SVD and DCT plus SVD based features. In addition, we employed MLSVMs to perform the fault classification. Since both the number of features and the σ values for the RBF kernel with MLSVMs can affect the classification accuracy, it is necessary to find the optimal values that yield the highest classification accuracy. Thus, we quantitatively estimated the optimal values of ($N_{feature}$-3) and σ by measuring the classification accuracies for varying values of ($N_{feature}$-3) and σ. To prove the improved

classification performance of the proposed SVD based feature extraction approaches, the proposed approaches were compared with two conventional methods. The experimental results indicated that the proposed approaches offered higher classification accuracies than two state-of-the-art techniques by achieving a true positive rate of more than 95%, even for noisy environments. Likewise, the features calculated using the DCT plus SVD technique fluctuated more than those calculated using the STE plus SVD technique in noisy environments, which indicates that the STE plus SVD feature extraction approach yields high classification accuracy in both noisy and noiseless environments.

Acknowledgments

This work was supported by the National Research Foundation of Korea (NRF) grant funded by the Korean government (MEST) (No. 2012R1A1A2043644).

References

[1] A.M. Da Silva, R.J. Povinelli, N.A.O. Demerdash, Induction machine broken bar and stator short-circuit fault diagnostics based on three-phase stator current envelopes, IEEE Transactions on Industrial Electronics Magazine 55 (2008) 1310–1318.
[2] S. Abbasion, A. Rafsanjani, A. Farshidianfar, N. Irani, Rolling element bearing multi-fault classification based on wavelet denosing and support vector machine, Mechanical Systems and Signal Processing 21 (2007) 2933–2945.
[3] P.A. Laggan, Vibration Monitoring, IEE Colloquium on Understanding Your Condition Monitoring, Chester, 1999, pp. 1–11.
[4] H. Han, S. Cho, U. Chong, Fault diagnosis system using LPC coefficients and neural network, in: Proceedings of International Forum on Strategic Technology, Ulsan, 2010, pp. 87–90.
[5] F.V. Nelwamonodo, T. Marwala, Fault detection using Gaussian mixture models, Mel-frequency Cepstral coefficients and Kurtosis, in: IEEE International Conference on Systems, Man and Cybernetics, Taipei, 2006, pp. 290–295.
[6] K.M. Silva, B.A. Souza, N.S.D. Brito, Fault detection and classification in transmission lines based on wavelet transform and ANN, IEEE Transactions on Power Delivery 21 (2006) 2058–2063.
[7] T. Boukra, A. Lebaroud, Classification on Induction Machine Faults, in: 2007 International Multi-Conference on Systems and Devices, Ammam, 2010, pp. 1–6.
[8] S. Poyhonen, Support Vector Machine Based Classification in Condition Monitoring of Induction Motors, Thesis Presented at Helsinki University of Technology, 2004.
[9] M. Deriche, Bearing fault diagnosis using wavelet analysis, in: 2005 International Conference on Computers, Communication and Signal Processing with Special Track on Biomedical Engineering, Kuala Lumpur, 2005, pp. 197–201.
[10] N. Mehla, R. Dahiya, An approach of condition monitoring of induction motor using MCSA, International Journal of System Application and Engineering Development 1 (2007) 13–17.
[11] F. Li, G. Meng, L. Ye, P. Chen, Wavelet transform-based higher-order statistics for fault diagnosis in rolling element bearings, Journal of Vibration and Control 14 (2008) 1691–1709.
[12] H. Ocak, K.A. Loparo, Estimation of the running speed and bearing defect frequencies of an induction motor from vibration data, Mechanical Systems and Signal Processing 18 (2004) 515–533.
[13] F.V. Nelwamonodo, T. Marwala, U. Mahola, Early classifications of bearing faults using hidden Markov models, Gaussian mixture models, Mel-frequency Cepstral coefficients and fractals, Journal of Innovative Computing, Information and Control 2 (2006) 1281–1299.
[14] M. Ge, G.C. Zhang, Y. Yu, Feature extraction from energy distribution of stamping processes using wavelet transform, Journal of Vibration and Control 8 (2002). (1323–1032).
[15] B.-S. Yang, K.J. Kim, Application of Dempster–Shafer theory in fault diagnosis of induction motors using vibration and current signals, Mechanical Systems and Signal Processing 20 (2006) 403–420.
[16] V.I. Gorodetski, L.J. Popyack, V. Samoilov, V.A. Skormin, SVD-based approach to transparent embedding data into digital images, in: Proceedings of International Workshop on Mathematical Methods, Models and Architecture for Computer Network Security 2052, 2001, pp. 263–274.
[17] L. Lu, H.-J. Zhang, H. Jiang, Content analysis for audio classification and segmentation, IEEE Transactions on Speech Audio and Processing 10 (2002) 504–516.
[18] D. Li, I.K. Sethi, N. Dimitrova, T. McGee, Classification of general audio data for content-based retrieval, Pattern Recognition Letters 22 (2001) 533–544.
[19] G. Strang, The discrete cosine transform, Journal of the Acoustical Society of America 41 (1999) 135–147.
[20] C.J.C. Burges, A tutorial on support vector machines for pattern recognition, Journal of Data Mining and Knowledge Discovery 2 (1998) 121–167.
[21] S.R. Gunn, Support Vector Machines for Classification and Regression, ISIS Technical Report, 1998.
[22] J. Zarei, Induction motors bearing fault detection using pattern recognition techniques, Expert Systems with Appilcations 39 (2012) 68–73.
[23] V.T. Do, U.–P. Chong, Signal model-based fault detection and diagnosis for induction motors using features of vibration signal in two-dimension domain, Journal of Mechanical Engineering 57 (2011) 655–666.